DOI: 10.17344/acsi.2018.4726 *Acta Chim. Slov.* **2019,** *66,* 136–144

Scientific paper

Fabrication of Silver-Modified Halloysite Nanotubes and their Catalytic Performance in Rhodamine 6G and Methyl Orange Reduction

Maryam Akhondi and Effat Jamalizadeh*

Department of Chemistry, Shahid Bahonar University of Kerman, Kerman, Iran.

** Corresponding author: E-mail: jamalizadeh@uk.ac.ir, jamalizadeheffat@yahoo.com. Tel./fax: +98 34 33257433*

Received: 09-12-2018

Abstract

Halloysite nanotube supported Ag nanoparticles (Ag/HNT) as catalyst for reduction of Rhodamine 6G (Rh6G) and Methyl orange (MO) have been synthesized and tested. 3-glycidyloxyproyltrimethoxysilane and Triethylene tetramine were successfully utilized to modify the HNTs surface, then Ag^+ ions were reduced to AgNPs on this functionalized HNT surface. The structure of AgNPs-impregnated HNT wall was characterized by FTIR, XRD, TEM, FE-SEM and EDX showing the AgNPs to be 10–15 nm in size. The catalytic activity of Ag/HNTs for Rh6G and MO reduction was investigated by UV-vis spectroscopy so as catalyzed and uncatalyzed reaction rate constants could be compared. The rate constant (k) of Rh6G and MO reduction was calculated for catalyzed reactions as 0.224 min^{-1} and 0.222 min^{-1}, and for un-catalyzed reactions as 0.049 min^{-1} and 0.014 min^{-1}, respectively. The Ag/HNT catalyzer was effectively recycled six times without appreciable loss of activity. Results indicate that supporting AgNPs on HNT surface functionalized with other compounds with superior performance in reducing Rh6G and MO dyes exist.

Keywords: Catalyst; Ag nanoparticles; Functionalized halloysite; GPTMS; TETA

1. Introduction

In recent years, great strides have been taken in use of metal nanomaterials as heterogeneous catalysts.[1–3] Nanomaterials have special properties such as the surface and interface effect which arise from the alteration of boundary between material and its surrounding, small size effect due to decrease in atom density of amorphous nanoparticles near the surface layer, quantum size effect arising from confinement of electrons to small regions of space in one, two, or three dimensions and also macroscopic quantum tunneling effect, leading to some new and potential applications such as catalysis, bio-engineering, medicine.[4–6] Industrial dye production and use apart from forming toxic by-products and non-biodegradable wastes that affect plants, animals and fish, are suspect as potential carcinogens.[7,8] Therefore, depending on the local laws and bylaws, to prevent environmental pollution, industrial wastewaters retaining organic dyes need treatment to remove the residual compounds. Various techniques for removal of dye molecules exist such as membrane filtration, ion exchange, biological treatment, coagulation-flocculation, ozone flashing, Fentons reagent.[9–13] The coagulation–flocculation process is widely used, due to its simplicity and cost-effectiveness,[9] however, it just transfers the dye molecules from liquid to solid form.[14] Catalysis as an efficient method to treat wastewater bearing colorants has attracted much interest.[15]

Among different type of metal nanoparticles, noble metal nanoparticles have attracted extensive attention as chemical catalyst.[16–18] Among these, Ag is particularly striking due to its remarkable catalytic activity and low cost. A significant number of studies on the catalytic reactions of Ag nanoparticles (AgNPs) have been reported, such as alcohol dehydrogenation,[19] oxidation of phenylsilanes,[20] reduction of aromatic compounds,[21] and Diels-Alder cycloadditions.[22] Since during a chemical reaction, the active surface atoms dislodge the AgNPs,[22–27] various supports such as polymeric[28,29] and inorganic materials, including silica,[30,31] zeolite,[32,33] alumina,[34,35] ceria,[36] titania,[37,38] zirconia,[39] activated carbon,[40,41] carbon nanotubes (CNTs),[42,43] and halloysite nanotubes (HNTs),[44–46] have been used to immobilize AgNPs. Halloysite silicate nanotubes of about 15 nm lumen, 50 nm external diameter and1000–2000 nm length are abundant in nature. Furthermore, HNTs are biocom-

patibile,[47,48] chemically stabale,[49] with high absorption capability[7] and potential to settle down quickly. HNTs ($Al_2Si_2O_5(OH)_4\ nH_2O$) have two-layered (1:1) aluminosilicate with aluminol (Al–OH) group in the internal and Si–OH group on the external surfaces. Presence of hydroxyl groups allows easy surface functionalization.[50–53] Existence of halloysite signicantly improves the size control of Ag nanoparticles as Ag nanoparticles without halloysite get to larger size and also aggregate heavily.[54] Nanotube supported Ag nanoparticles (Ag/HNT), are used with various precursors and for different applications such as biosensor,[55–56] polymerization catalyst,[44] photocatalyst,[45,46] enzyme immobilization,[55] dielectric material[57] and antibacterial usage.[58,59] In addition, the Ag/HNTs show high catalytic activity even at minute amounts towards reduction and degradation of some industrial dyes, 4-nitrophenol[60–62] or methylene blue.[62]

The purpose of this paper is to enhance the catalytic effect of Ag nanoparticles as a heterogeneous catalyst to reduce 6G Rh6G and MO dyes by supporting them on the walls of halloysite nanotubes modified with new compounds. Such modification of the external surface of HNTs was achieved, and then in situ reduction of Ag^+ to Ag nanoparticles on the functionalized HNTs surface resulted in synthetized Ag/HNTs which was then utilized as a heterogeneous catalyst in the degradation of Methyl orange and Rhodamine 6G in aqueous solution (Fig. 1). The recyclability of the Ag/HNTs catalyst was tested by carrying out repeated runs of the same reaction system.

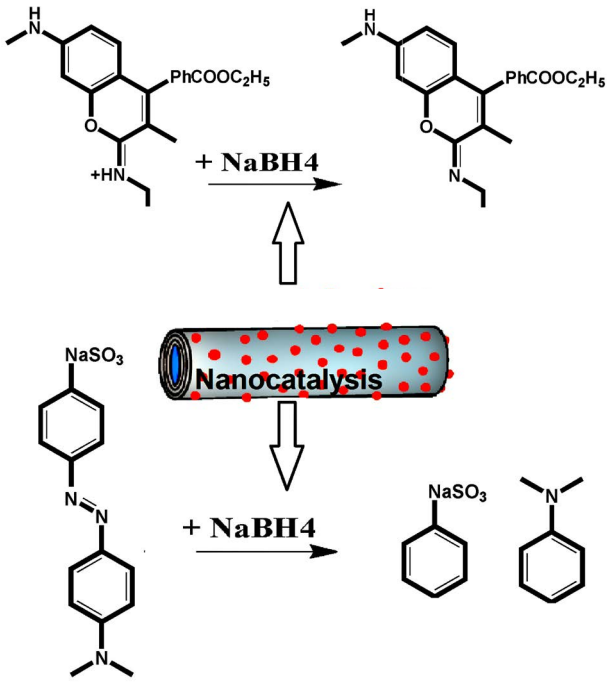

Fig 1. Reduction of Rh6G and MO by $NaBH_4$ catalyzed by the Ag/HNT.

2. Methods

2. 1. Materials

The halloysite nanotube powder was provided by New Zealand China Clays Ltd., Auckland, New Zealand. The Sodium borohydride ($NaBH_4 \geq 99.99\%$), Sodium hydroxide ($NaOH \geq 97.00\%$) and hydrochloric acid ($HCl \geq 37.00\%$) were acquired from the Sigma Aldrich. The silver nitrate ($AgNO_3 \geq 99\%$), 3-glycidyloxyproyltrimethoxysilane (GPTMS ≥ 98%), Triethylene tetramine (TETA), Ethanol, MO and Rh6G were purchased from Merck.

2. 2. Instruments

UV-vis spectra were recorded on a spectrophotometer (Varian, Cary50), with a quartz cuvette (1.0 cm path length, and 4 mL volume). Scanning electron microscope images were obtained with a field-emission scanning electron microscope (FE-SEM) KYKT, EM-3200. Transmission Electron Microscope (TEM) images were recorded from JEOL 2100F TEM. XRD patterns were obtained in reflection mode using a powder X-ray diffractometer (X'Pert Pro MPD Philips X-ray diffractometer (Ni-filtered Cu-Kα radiation, λ = 0.154 nm). FT-IR spectra of samples as KBr discs were recorded on a FT-IR 8400-Shimadzu in the range 400–4000 cm^{-1}. The pH measurements were performed using a pH-meter (METROHM, Model 713).

2. 3. Functionalization of HNTs

As shown in Fig 2, for functionalization of HNTs by grafting the GPTMS containing epoxy groups on the surface of HNTs via silanization; 1 mL of GPTMS was added to 0.5g of HNTs dispersed in 7 mL of ethanol and was stirred at 65 °C for 24 h and then centrifuged to collect the suspension. The precipitate (GPTMS/HNT) was washed five times with pure ethanol and dried at 60 °C for 10 h. Following that, TETA was grafted on tubes via ring opening reaction of epoxy groups by adding 6mL of pure ethanol containing TETA (0.1 mg L^{-1}) to 0.5 g of GPTMS/HNTs, stirred and refluxed for 24 h at 70 °C. This mixture was then centrifuged and the precipitate (TETA/HNT) was again washed with ethanol five times, dried at 70 °C for 10 h.

2. 4. Synthesis of Ag/HNTs Nanocomposite

The Ag/HNT composite was prepared using $AgNO_3$ as silver precursor, so that silver ions get reduced to silver nanoparticles on TETA/HNT's surface amine functional groups. In a typical synthesis process, 0.5 g of TETA/HNTs was added to 10 mL of deionized water under stirring for 1 h and then, 1 mL of 0.2 M $AgNO_3$ solution was added dropwise to the mixture and left stirring for 30 min. The solution was reduced by addition of 2 mL of freshly pre-

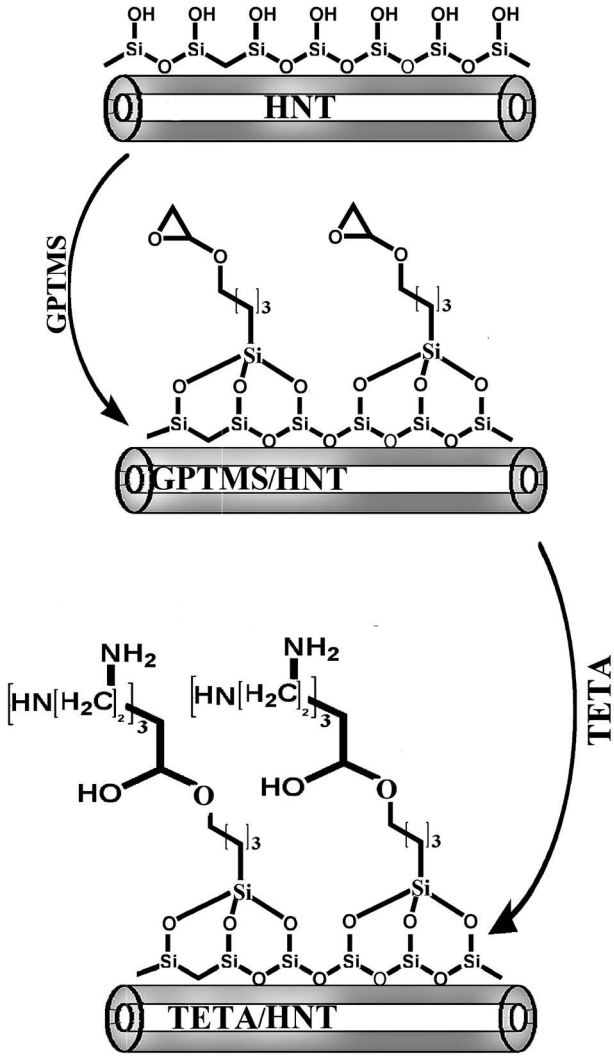

Fig 2. Schematic Illustration of the role of GPTMS and TETA in the formation of the TETA/HNTs.

pared 0.1 M aqueous $NaBH_4$ solution. The color of the reaction mixture turns from white to dark green, indicating formation of Ag NPs on the surface of HNTs (Ag/HNTs). The final product was washed several times with de-ionized distilled water to remove unreacted Ag^+ ions and any byproducts. All experiments were performed at room temperature.

2. 5. Catalytic Reduction of Dyes by Ag/HNTs Nanocomposite

Catalytic activity of Ag/HNTs nanocomposite, on decomposing Rh6G and MO dyes was investigated by comparing the rate they reacted with $NaBH_4$ in the presence and absence of nanocomposite. The reduction of dyes was carried out in the quartz cell by admixing 1.0 mL of 1mM $NaBH_4$ as reducing agent to a mixture of 2 mL of aqueous dye solution and 1 mg of Ag/HNTs nanocomposite. The process was continuously monitored by a UV–vis spectroscopy at room temperature. In order to determine its reusability after the reaction was over, the Ag/HNT catalyst was centrifuged and washed with deionized water for two times, and dried in vacuum for 24 h at 50 °C, to be used again in dye decomposition processes.

The reduction of Rh6G and MO with an excess amount of $NaBH_4$ has been used as a model reaction to examine the catalytic performance of the Ag/HNTs.

The reaction kinetics can be described as Eq. (1):[40]

$$\ln(C/C_\circ) = -kt \quad (1)$$

where C° is the initial concentration of dye, C is the concentration of dye at time t, k is the apparent first-order rate constant (min^{-1}), and t is the time. Since the concentration of a solution is proportional to its adsorption, Eq. (1) can be written as follow:

$$\ln(A/A_\circ) = -kt \quad (2)$$

$A_\circ$ and A are respectively, the initial and time t dye adsorption.

Degradation efficiency (%D) of Ag/HNT is calculated according to the following Eq. (3):

$$\%D = \frac{A_0 - A}{A_0} \times 100 \quad (3)$$

Rh6G and MO reduction was investigated under various solution pH values of 3, 5, 7, 9 and 11 using sodium hydroxide and hydrochloric acid were also performed.

3. Results and Discussion

3. 1. FTIR Spectra

The FTIR spectra were used to determine the chemical structure of the HNTs during the functionalization process. As shown in Fig 3, the characteristic peaks of HNTs occurs at 3698 cm^{-1} and 3623 cm^{-1}; attributable to O–H stretching of hydroxyl groups.[63] Peaks observed at 1109 cm^{-1} and 1034 cm^{-1} are ascribed to in-plane stretching of Si–O bond.[63] FTIR of the modified halloysite with GPTMS (GPTMS/HNT) shows new peaks at 2925 and 2854 cm^{-1}, which is assigned to the asymmetric and symmetric stretching vibration of aliphatic $–CH_2$ groups. This can also confirm the existence of GPTMS grafted on the HNTs.[64] For GPTM/halloysite grafted by TETA (TETA/HNT), in addition to the presence of CH_2 bands at 2946 cm^{-1} and 2871 cm^{-1}, there are also two new peaks at 1200 and 1600 cm^{-1}, belonging to the C-N and NH_2 groups, respectively.[65] These results can also show the interaction between TETA and epoxide ring of GPTMS grafted on the HNTs indicating tghat nanotubes have been successfully functionalized with amine groups. In comparing these results with the FTIR spectra of pure HNTs, the positions of

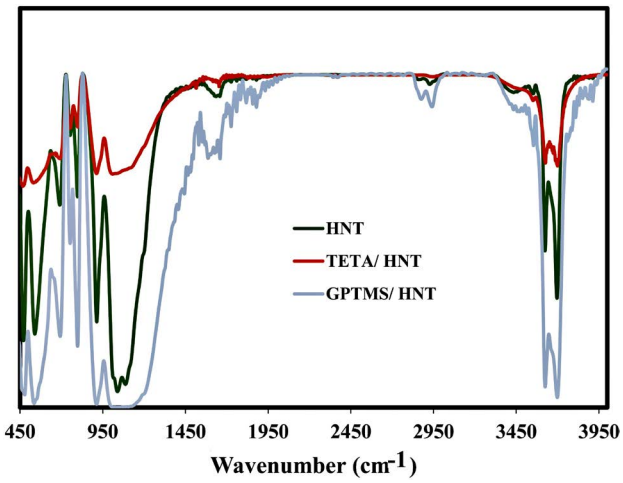

Fig 3. FT-IR spectra of HNTs, GPTMS/HNTs and TETA/HNTs.

most HNT peaks do not show any change, demonstrating preservation of main structure of HNT following GPTMS and TETA grafting.

3. 2. UV-vis Spectra

Fig 4 shows the UV-vis optical absorption spectra of the HNTs and Ag/HNTs in the 200–800 nm spectral range. The UV-vis spectra of HNTs dispersed in water revealed no absorption band, while the Ag/HNTs sample revealed an absorption band in 427 nm, corresponding to the surface plasmon resonance (SPR) of Ag nanoparticles.

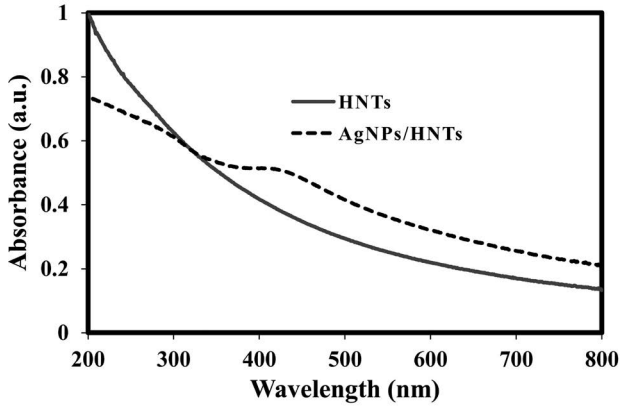

Fig 4. UV–vis spectra of HNTs and Ag/HNTs.

3. 3. FE-SEM and EDX Analysis

The FE-SEM image of HNTs and Ag/HNTs are shown in Figs 5(a) and 5(b). The diameter of the HNTs particles are about 123 nm with random length. Fig 5 shows the halloysite nanotubes along with some non-tubolar structures. The particles of halloysite can adopt a multifariousness of morphologies, the most common of which is the elongated tube. However, short tubular, spheroidal and plate shapes have all been widely reported.[66–68] The Ag nanoparticles are almost unobservable in Fig 5(b) but EDX analysis confirms the existence of Ag element on the surface of halloysites.

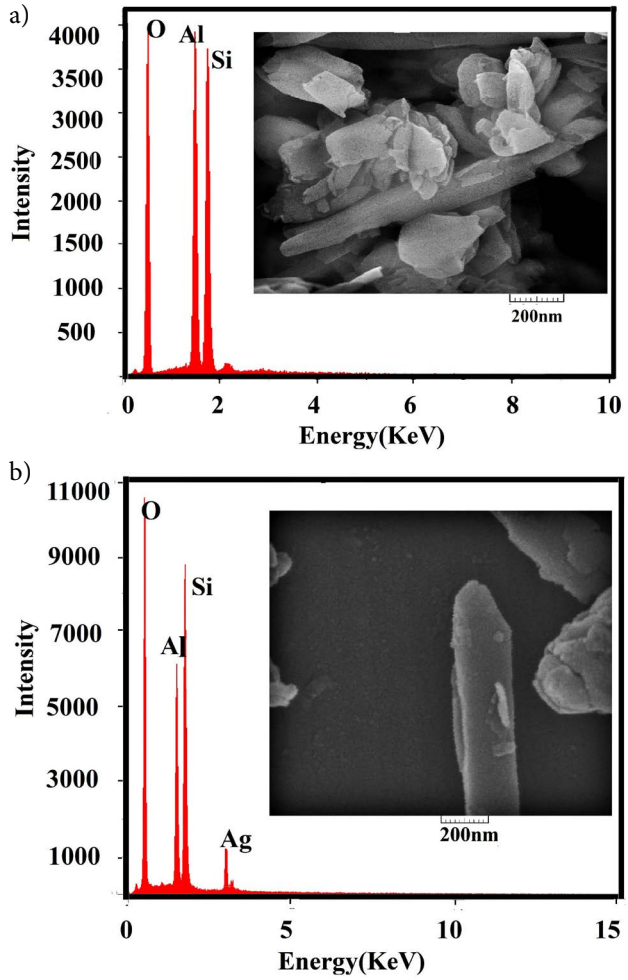

Fig 5. EDX spectra and FE-SEM images of (a) HNTs and (b) Ag/HNTs.

3. 4. TEM Analysis

TEM image of structure and morphology of Ag/HNTs is shown in Fig 6. This reveals the hollow open ended tubular morphology of HNTs with the inner and outer

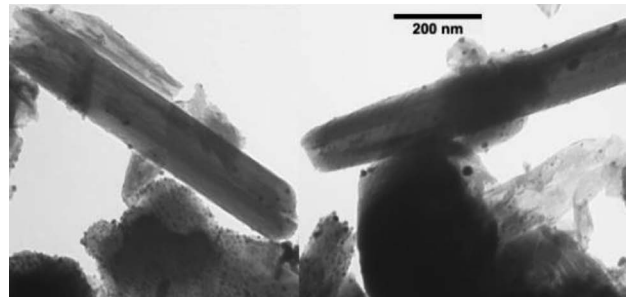

Fig 6. TEM image of Ag/HNTs.

diameters of about 15–40 nm and 50–140 nm, respectively. It also shows spherical single nanoparticles with average size of 10 nm dispersed evenly, indicating that amine terminated groups had adsorbed Ag^+ ions from solution.

3. 5. X-ray Diffraction Analysis

The X-ray diffraction (XRD) pattern of HNTs and Ag/HNTs are shown in Fig 7. The XRD patterns of the functionalized HNT reveal well defined diffraction peaks all corresponding to the HNT, confirming that modification with GPTMS and TETA does not affect the structure of the HNT. However, in the XRD pattern of the Ag/HNTs nanocomposite, four new peaks at 2θ value of 37.7°, 43.5°, 64.2° and 77.4° emerge which are ascribed to (1 1 1), (2 0 0), (2 2 0) and (3 1 1) reflections of FCC structure of silver;[46,69] so this further affirming successful attachment of AgNPs to the surface of the nanotubes.

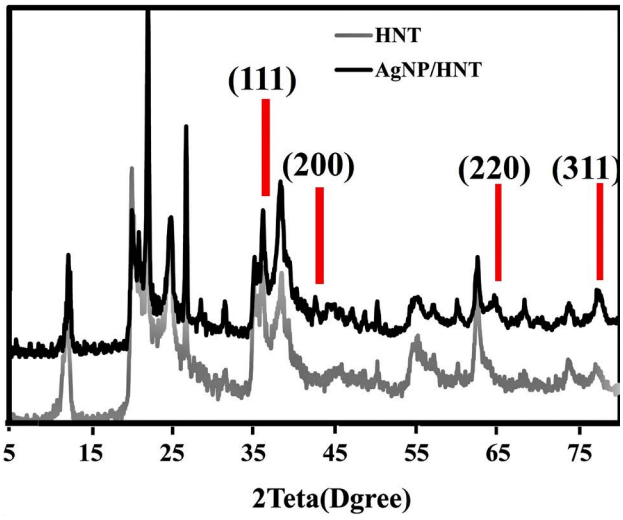

Fig 7. XRD pattern of HNTs and Ag/HNTs.

3. 6. Catalytic Reduction of Rh6G and MO

The results of catalytic activity of synthesize Ag/HNTs in reduction of Rhodamine 6G and methyl orange studied by UV–visible spectrophotometry are shown in Figs 8 and 9. Time dependent reduction of Rh6G and MO with $NaBH_4$ in presence and absence of Ag/HNTs was observed by the successive decrease in the absorbance value at 516 and 467 nm, respectively. Results indicate that the reduction of Rh6G and MO in absence of catalyst at room temperature occurs which is greatly enhanced by addition of Ag/HNTs. Fig 8, exhibits a rapid Rh6G concentration decay in presence of Ag/HNTs in 12 min ($\Delta OD_{12\ min} = 0.4$), compared to sluggish 30 min un-catalyzed reaction ($\Delta OD_{30\ min} = 0.4$). Similarly, Fig 9, demonstrates rapid decay of MO in presence of Ag/HNTs in just 12 min ($\Delta OD_{12\ min} = 0.8$), compared to its slow degradation needing 30 min when relying on un-catalyzed reaction ($\Delta OD_{30\ min} = 0.34$). It is observed that degradation of methyl orange is classically enhanced in presence of silver nanoparticles due to electron relay effect.[25, 26]

As presented in Table 1, the rate constant (k) of Rh6G and MO degradation has been calculated for catalyzed reactions as 0.224 min^{-1} and 0.222 min^{-1}, and for un-catalyzed reactions as 0.049 min^{-1} and 0.014 min^{-1}, respectively.

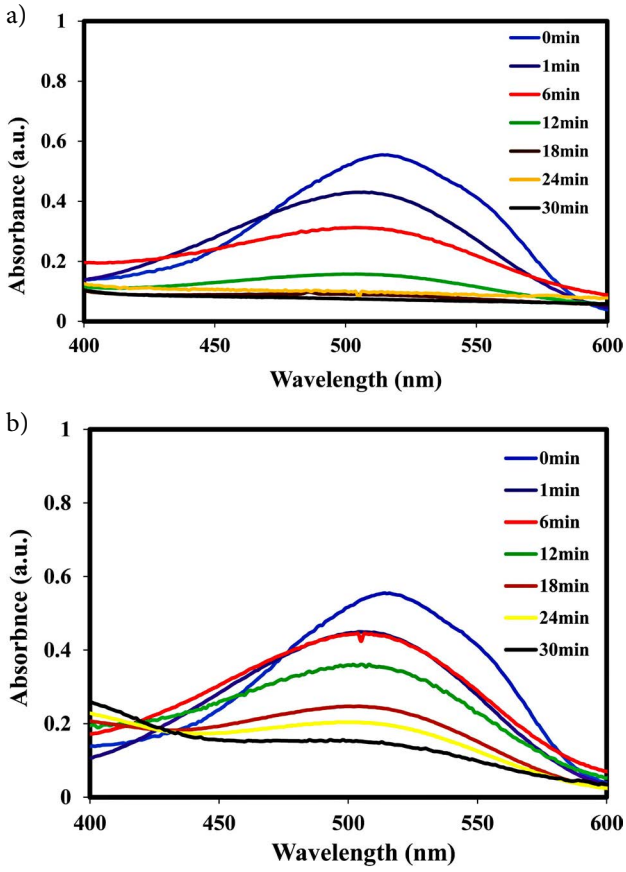

Fig 8. Time-dependent UV-vis absorption spectra for the reduction of Rh6G with $NaBH_4$ (a) in the presence and (b) absence of Ag/HNTs at room temperature.

3. 7. Effect of Amount of Catalyst

The amount of catalysts is an important factor affecting suitability of a catalyst for chemical reactions. Tables 2 and 3 present the optimization of degradation conditions for Rh6G and MO in early times. The Ag/HNTs catalyst amount was varied in 0.0002 g L^{-1} to 0.0025 g L^{-1} range at constant $NaBH_4$ concentration of 4 mg L^{-1} and dye concentration of 10 mg L^{-1}. According to the results, the rate of catalytic degradation of both dyes increased with increase in the amount of catalyst. This is due to the increase in the number of surface active sites and increased dye molecules adsorption on the catalyst surface.[25]

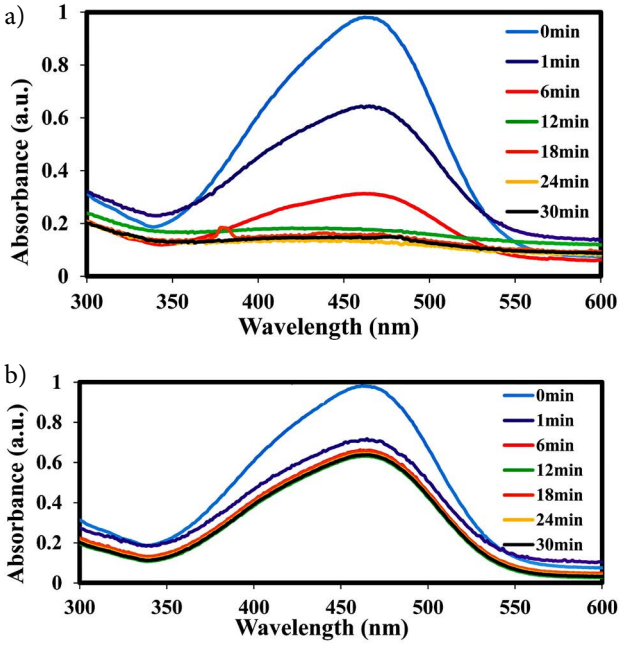

Fig 9. Time-dependent UV-vis absorption spectra for the reduction of MO with $NaBH_4$ (a) in presence and (b) absence of Ag/HNTs at room temperature.

3. 8. Effect of Amount of $NaBH_4$

In order to evaluate the effect of $NaBH_4$ concentration on degradation of dyes, this was varied the in the range of 1.5 to 16 g L^{-1}, while keeping dye concentration at 10 mg L^{-1} and Ag/HNT concentration at 0.001 g L^{-1}. Tables 2 and 3 show that with one exception, the increase in $NaBH_4$ concentration, increases degradation of both dyes, due to higher number of electrons which promotes the simultaneous reduction of the Ag particles from its oxide and the reduction of dyes.[25] However, as mentioned, the rate constant for the 8 g L^{-1} concentration of $NaBH_4$ is observed to decrease. This is caused by excessive production of electrons from the ion leading to the saturation of electrons[70] leaving AgNPs incapable of relaying the electrons.

The catalytic reduction of dyes in the presence of $NaBH_4$ on the surface of noble metal nanoparticles is considered to follow Langmuir–Hinshelwood mechanistic pathway,[62,71] as Fig 10 demonstrates, these dyes are electrophilic with respect to Ag NPs and nucleophilic toward BH^-_4. Thus both dyes and BH^-_4 are adsorbed on the surface of AgNPs attached to the surface of HNTs. The fast nature of adsorption on the surface of nanoparticles and its reversibility has been reported.[62,71,72] When $NaBH_4$ is added to the reaction solution, the hydride from $NaBH_4$ may be trapped by AgNPs and get adsorbed on the surface transfering its electron to the AgNPs. Following this electron exchange, a hydrogen atom is formed from BH^-_4 that subsequently attacks any nearby dye molecule, and a spontaneous electron transfer-induced hydrogenation of the dye occurs. In fact, a negatively charged AgNP may be regarded as a nano-electrode at a negative potential which is trying to release its extra electrons which are finally released to dye molecule as an electron acceptor producing its reduced form.[71,73] AgNPs on the surface of HNTs significantly increases the rate of catalytic reduction due to lower work function of Ag (4.26 eV) and its tendency to release electron more easily even compared to the other noble metals.[62,74] Both nanoparticle's surface area and heterogeneous organic–inorganic hybrid structure supporting for AgNPs may contribute to reduction rate by increasing adsorption ability of reactant.[62]

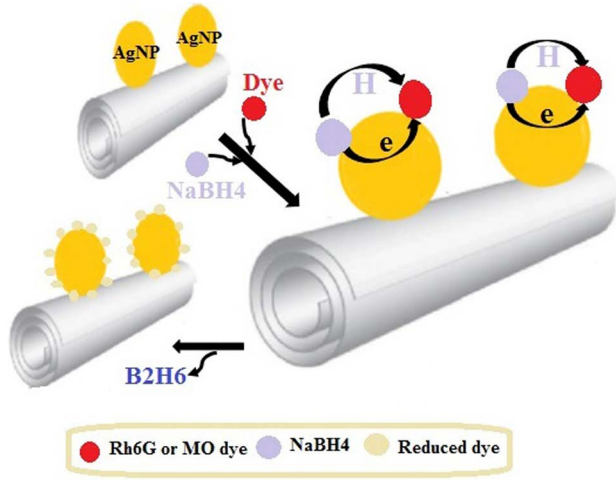

Fig 10. Proposed mechanism of reduction of dyes by catalytic sample.

3. 9. Effect of pH

The solution pH has significant effect on degradation of organic dyes. Fig 11 shows the reduction of MO and Rh6G at pH 3, 5, 7, 9, and 11 after 20 min. It was observed that the percentage of degradation of both dyes increased with decreasing pH from 7 to 3, and conversely, degradation fall at pH 9 and 11. The results show decreasing Rh6G solution pH from 7 to 3, increases the degradation efficiency from 78.0% to 79.7% while, pushing pH towards 11 decrease it to 73.6%. Similarly, decomposition of MO goes up from 73.9% to 77.1 % by reducing pH from 7 to 3 and solution pH of 11, cuts it to 70.6 %. In acidic media the MO molecules (pK_a = 3.4) undergo protonation[74,75] and the resulted protonated molecules are adsorbed better on negatively charged AgNPs, enhancing MO degradation. Similarly, the lower degradation rate observed for Rh6G at higher pH may attributed to the deprotonation of the Rh6G in alkaline solution since Rhodamine 6G (pK_a = 7.5) is a weak base and can easily lose proton under the effect of a strong base, which leads to partial neutralization of its positive charge.[76] As a result, electrostatic interaction with negatively charged Ag/HNT decreases decreasing the overall Rh6G degradation.

Table 4 summaries the dye reduction studies reported in literature. The synthesized Ag/HNTs while perform-

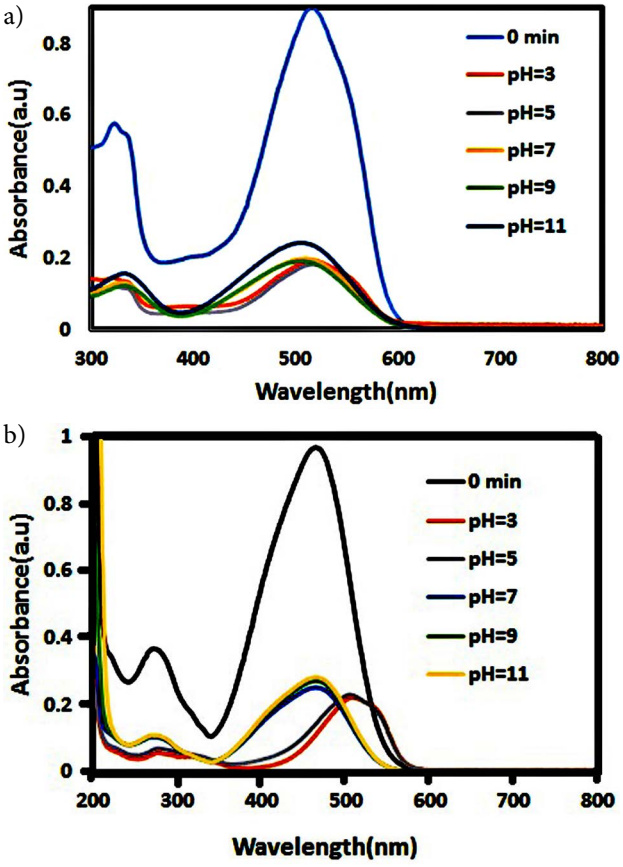

Fig 11. Time-dependent UV-vis absorption spectra for the reduction (a) Rh6G and (b) MO with $NaBH_4$ in presence of Ag/HNTs at different pH values.

ing on par with other Ag catalysts for the degradation of MO and Rh6G.[25,77–79] although, the K value in this work is 0.21 min^{-1} which is slightly lower compared to the Ag supported on zeolite (0.30 min^{-1}),[77] it has the advantage of using much smaller amounts of Ag. In the present work, amount of used Ag/HNTs as catalyst is 2.4 times less than the AgNPs/Zeolite X, hence, the Ag/HNT catalysis would be more economical compared to the other catalysts reported in Table 4.[25,78] not only because of low concentrations used but also due to the easy recovery and reusability. The halloysite as a natural mineral with high stability as support material for Ag nanoparticles, while Zeolite X[77] is not natural and its preparation is costly. Also, although the Ag/tannic acid membrane[79] has inner shell as natural substrate but this substrate is unstable.

3. 10. Reusability of the Synthesized Catalysts

The environment impact by catalysts such as heavy metals which should include recovery and recycling is an important factor in choosing a catalyst.[80] Due to the one-dimensional nature of Ag/HTNs its use as a recyclable and reusable catalysts which is easily recovered from the reaction mixture by simple filtration is very advantageous.

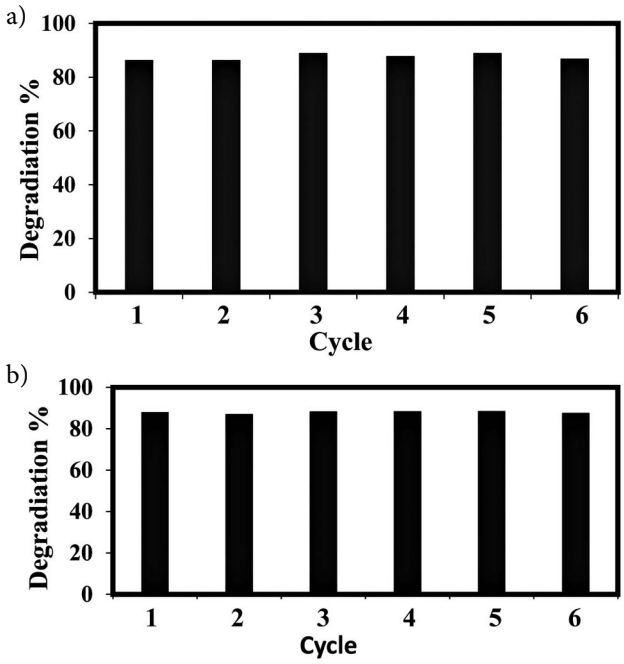

Fig 12. Recyclability and reusability of the synthesized Ag/HNTs for the reduction of Rh6G and MO.

The recycling experiments involving synthesized Ag/HNTs for reduction of MO and Rh6G are shown in Fig 12. The data show that the Ag/HNT catalyst could be repeatedly used for at least six times and still maintained degradation potency of over 85. Overall, Ag/HNT as a dye decomposing catalyst has a high operational stability with no appreciable loss in catalytic activity and good reusability.

4. Conclusion

Halloysite nanotube supported Ag nanoparticles synthesized in situ by reduction of silver ions on the amine functional groups on the surface of TETA/HNTs greatly improves dispersion and stability of the Ag nanoparticles on HNT surfaces. The Ag/HNTs exhibit good catalytic activity in decomposition of MO and Rh6G by $NaBH_4$ as the reducing agent. The catalytic efficiency was enhanced with the increasing amount of Ag/HNTs. Notably, the Ag/HNTs could be easily recycled due to the one-dimensional nanostructural property. These results signify that Ag nanoparticles strongly attached and immobilized on the surface of halloysite modified with GPTMS and TETA increase silver performance as Rh6G and MO dyes decomposer.

5. References

1. D. Kumar Dutta, B. Jyoti Borah and P. Pollov Sarmah, *Catal Rev.* **2015**, *57*, 257–305.
DOI:10.1080/01614940.2014.1003504

2. T. Yasukawa, A. Suzuki, H. Miyamura, K. Nishino and S. Kobayashi, *J. Am. Chem. Soc*. **2015**, *137,* 6616–6623. **DOI:**10.1021/jacs.5b02213
3. S. Zhang, X. Shen, Z. Zheng, Y. Ma and Y. Q*u, J. Mater. Chem. A***. 2015**, *3,* 10504–10511. **DOI:**10.1039/C5TA00409H
4. J. Wang and H. Gu, *Molecules.* **2015**, *20,* 17070–17092. **DOI:**10.3390/molecules200917070
5. V. Pareek, A. Bhargava, R. Gupta, N. Jain and J. Panwar, *Adv. Sci. Eng. Med.* **2017**, *9,* 527–544. **DOI:**10.1166/asem.2017.2027
6. K. W. Choi, D. Y. Kim, S. J. Ye and O. O. Park, *Adv. Mater. Res.* **2014**, *3,* 199–216. **DOI:**10.12989/amr.2014.3.4.199
7. P. Velusamy, S. Pitchaimuthu, S. Rajalakshmi and N. Kannan, *J. Adv. Res.* **2014**, *5,* 19–25. **DOI:**10.1016/j.jare.2012.10.001
8. H. R. Pouretedal, H. Eskandari, M. H. Keshavarz and A. Semnani, *Acta Chim. Slov.* **2009**, *56*. **2007**, *2*, 14–18.
9. A. K. Verma, R. R. Dash and P. Bhunia, *J. Environ. Manage.* **2012**, 93, 154–168.S. Mostafa, F. Behafarid, J. R. Croy, L. K. Ono, L. Li, J. C. Yang, A. I. Frenkel and B. R. Cuenya, *J. Am. Chem. Soc.* **2010**, *132,* 15714–15719.
10. T. Poznyak, P. Colindres and I. Chairez, *J. Mex. Chem. Soc.* **2007**, *51,* 81–86.
11. C. Thamaraiselvan and M. Noel, *Crit Rev Env Sci Tec.* **2015**, *45,* 1007–1040. **DOI:**10.1080/10643389.2014.900242
12. P. Palaniandy and S. F. AHBA, *Int. j. innov. eng.* **2014**, *2*.
13. S. Karcher, A. Kornmüller and M. Jekel, *Water Res*. **2002**, *36,* 4717–4724. **DOI:**10.1016/S0043-1354(02)00195-1
14. S. Rajalakshmi, S. Pitchaimuthu, N. Kannan and P. Velusamy, *Appl Water Sci.* **2017**, *7,* 115–127. **DOI:**10.1007/s13201-014-0223-5
15. B. K. Ghosh and N. N. Ghosh, *J. Nanosci. Nanotechnol.* **2018**, *18,* 3735–3758. **DOI:**10.1166/jnn.2018.15345
16. B. Hvolbæk, T. V. Janssens, B. S. Clausen, H. Falsig, C. H. Christensen and J. K. Nørskov, *Nano Today.* **2007**, *2,* 14–18. **DOI:**10.1016/S1748-0132(07)70113-5
17. F. P. da Silva, J. L. Fiorio and L. M. Rossi, *ACS Omega.* **2017**, *2,* 6014–6022.
18. S. Mostafa, F. Behafarid, J. R. Croy, L. K. Ono, L. Li, J. C. Yang, A. I. Frenkel and B. R. Cuenya, *J. Am. Chem. Soc.* **2010**, *132,* 15714–15719. **DOI:**10.1021/ja106679z
19. T. Mitsudome, Y. Mikami, H. Funai, T. Mizugaki, K. Jitsukawa and K. Kaneda, *Angew. Chem. Int. Ed.* **2008**, *120,* 144–147. **DOI:**10.1002/ange.200703161
20. T. Mitsudome, S. Arita, H. Mori, T. Mizugaki, K. Jitsukawa and K. Kaneda, *Angew. Chem. Int. Ed.* **2008**, *120,* 8056–8058. **DOI:**10.1002/ange.200802761
21. P. Zhang, C. Shao, Z. Zhang, M. Zhang, J. Mu, Z. Guo and Y. Liu, *Nanoscale.* **2011**, *3,* 3357–3363. **DOI:**10.1039/c1nr10405e
22. N. Pradhan, A. Pal and T. Pal, *Colloids Surf. A: Physicochem. Eng. Asp.* **2002**, *196,* 247–257. **DOI:**10.1016/S0927-7757(01)01040-8
23. L.-Q. Zheng, X.-D. Yu, J.-J. Xu and H.-Y. Chen, *Chem. Commun.* **2015**, *51,* 1050–1053. **DOI:**10.1039/C4CC07711C
24. V. Vidhu and D. Philip, *Spectrochim. Acta A*. **2014**, *117,* 102–108. **DOI:**10.1016/j.saa.2013.08.015
25. B. Vellaichamy and P. Periakaruppan, *RSC Adv.* **2016**, *6,* 31653–31660.
26. N. Isa, S. H. Sarijo, A. Aziz and Z. Lockman: AIP Conference Proceedings, AIP Publishing, **2017**, pp. 070001.
27. A. Rajan, V. Vilas and D. Philip, *J. Mol. Liq.* **2015**, *207,* 231–236. **DOI:**10.1016/j.molliq.2015.03.023
28. S. Patra, A. N. Naik, A. K. Pandey, D. Sen, S. Mazumder and A. Goswami, *Appl Catal A-Gen.* **2016**, *524,* 214–222. **DOI:**10.1016/j.apcata.2016.07.001
29. N. P. B. Tan, C. H. Lee and P. Li, *J. Polym.* **2016**, *8,* 105.
30. Z.-J. Jiang, C.-Y. Liu and L.-W. Sun, *J. PHYS. CHEM. B.* **2005**, *109,* 1730–1735. **DOI:**10.1021/jp046032g
31. Z. Qu, W. Huang, M. Cheng and X. Bao, *J. PHYS. CHEM. B.* **2005**, *109,* 15842–15848. **DOI:**10.1021/jp050152m
32. Y. Wu, C. Li, J. Bai and J. Wang, Results in physics. **2017**, *7,* 1616–1622.
33. M. Choi, Z. Wu and E. Iglesia, *J. Am. Chem. Soc.* **2010**, *132,* 9129–9137. **DOI:**10.1021/ja102778e
34. R. Poreddy, E. J. García-Suárez, A. Riisager and S. Kegnæs, *Dalton Trans.* **2014**, *43,* 4255–4259. **DOI:**10.1039/C3DT52499J
35. B. Naik, V. S. Prasad and N. N. Ghosh, *Powder Technol.* **2012**, *232,* 1–6. **DOI:**10.1016/j.powtec.2012.07.052
36. M. J. Beier, T. W. Hansen and J.-D. Grunwaldt, J. Catal. **2009**, *266,* 320–330. **DOI:**10.1016/j.jcat.2009.06.022
37. S. Deshmukh, R. Dhokale, H. Yadav, S. Achary and S. Delekar, *Appl Surf Sci.* **2013**, *273,* 676–683. **DOI:**10.1016/j.apsusc.2013.02.110
38. H. Sakai, T. Kanda, H. Shibata, T. Ohkubo and M. Abe, *J. Am. Chem. Soc.* **2006**, *128,* 4944–4945. **DOI:**10.1021/ja058083c
39. L. Kundakovic and M. Flytzani-Stephanopoulos, *Appl Catal A-Gen.* **1999**, *183,* 35–51. **DOI:**10.1016/S0926-860X(99)00043-5
40. L. Ai and J. Jiang, *Bioresour Technol.* **2013**, *132,* 374–377. **DOI:**10.1016/j.biortech.2012.10.161
41. H. Le Pape, F. Solano-Serena, P. Contini, C. Devillers, A. Maftah and P. Leprat, Carbon. **2002**, *40,* 2947–2954. **DOI:**10.1016/S0008-6223(02)00246-4
42. S. Ma, R. Luo, J. I. Gold, Z. Y. Aaron, B. Kim and P. J. Kenis, *J. Mater. Chem. A*. **2016**, *4,* 8573–8578. **DOI:**10.1039/C6TA00427J
43. Y. Liu, G. Wu and Y. Cui, *Appl. Organomet. Chem.* **2013**, *27,* 206–208. **DOI:**10.1002/aoc.2950
44. C. Li, X. Li, X. Duan, G. Li and J. Wang, *Journal of Colloid and Interface Science*. **2014**, *436*, 70–76. **DOI:**10.1016/j.jcis.2014.08.051
45. I. Fatimah and R. Herianto, *Oriental Journal of Chemistry.* **2018**, *34*, 857–862.
46. M. Zou, M. Du, H. Zhu, C. Xu and Y. Fu, *Journal of Physics D: Applied Physics.* **2012**, *45*, 325302. **DOI:**10.1088/0022-3727/45/32/325302
47. V. Vergaro, E. Abdullayev, A. Zeitoun, G. Giovinazzo, A. Santino, R. Cingolani, Y. M. Lvov and S. Leporatti, *J. Microencapsul.* **2008**, *25,* 376.
48. D. Mills, *Faseb J.* **2014**, 28, 87.4.
49. R. D. White, D. V. Bavykin and F. C. Walsh, *Nanotech.* **2012**,

23, 065705. **DOI:**10.1088/0957-4484/23/6/065705
50. P. Sudhakar and H. Soni, J Environ Chem Eng. **2018**, *6,* 28–36.
51. E. Abdullayev and Y. Lvov, *J. Nanosci. Nanotechnol.* **2011**, *11,* 10007–10026. **DOI:**10.1166/jnn.2011.5724
52. P. Sun, G. Liu, D. Lv, X. Dong, J. Wu and D. Wang, *J. Appl Polym Sci.* **2016**, 133.
53. J. Zhang, Y. Zhang, Y. Chen, L. Du, B. Zhang, H. Zhang, J. Liu and K. Wang, *Ind Eng Chem Res*. **2012**, *51,* 3081–3090. **DOI:**10.1021/ie202473u
54. S. Li, F. Tang, H. Wang, J. Feng and Z. Jin, *RSC Advances*. **2018**, *8*, 10237–10245. **DOI:**10.1039/C8RA00423D
55. S. Kumar-Krishnan, A. Hernandez-Rangel, U. Pal, O. Ceballos-Sanchez, F. Flores-Ruiz, E. Prokhorov, O. A. de Fuentes, R. Esparza and M. Meyyappan, *Journal of Materials Chemistry B*. **2016**, *4*, 2553–2560. **DOI:**10.1039/C6TB00051G
56. D. Rawtani, Y. Agrawal and P. Prajapati, *BioNanoScience*. **2013**, *3*, 73–78. **DOI:**10.1007/s12668-012-0071-4
57. Y. Ren, S. Zhang, X. Wan, Y. Zhan, J. Zhang and Y. He, *Polymer Engineering & Science*. **2018**, *58,* 2227–2236. **DOI:**10.1002/pen.24840
58. S. Jana, A. V. Kondakova, S. N. Shevchenko, E. V. Sheval, K. A. Gonchar, V. Y. Timoshenko and A. N. Vasiliev, *Colloids and Surfaces B: Biointerfaces*. **2017**, *151*, 249–254. **DOI:**10.1016/j.colsurfb.2016.12.017
59. Y. Zhang, Y. Chen, H. Zhang, B. Zhang and J. Liu, *Journal of inorganic biochemistry*. **2013**, *118*, 59–64. **DOI:**10.1016/j.jinorgbio.2012.07.025
60. X. Zeng, Q. Wang, H. Wang and Y. Yang, *Journal of Materials Science*. **2017**, *52*, 8391–8400. **DOI:**10.1007/s10853-017-1073-y
61. P. Liu and M. Zhao, *Applied Surface Science.* **2009**, *255*, 3989–3993. **DOI:**10.1016/j.apsusc.2008.10.094
62. T. K. Das, S. Ganguly, P. Bhawal, S. Remanan, S. Mondal and N. Das, *Applied Nanoscience.* **2018**, *8,* 173–186. **DOI:**10.1007/s13204-018-0658-3
63. H. Zhu, M. Du, M. Zou, C. Xu and Y. Fu, *Dalton Trans.* **2012**, *41,* 10465–10471. **DOI:**10.1039/c2dt30998j
64. E. K. Kim, J. Won, J.-y. Do, S. D. Kim and Y. S. Kang, *J. Cult Herit.* **2009**, *10,* 214–221. **DOI:**10.1016/j.culher.2008.07.008
65. H.-T. Lu, *Colloid J.* **2013**, *75,* 311–318. **DOI:**10.1134/S1061933X13030125
66. E. Joussein, S. Petit, J. Churchman, B. Theng, D. Righi and B. Delvaux, De Gruyter, **2005**.
67. S. Levis and P. Deasy, *Int J Pharm.* **2002**, *243,* 125–134. **DOI:**10.1016/S0378-5173(02)00274-0
68. B. Theng, M. Russell, G. Churchman and R. Parfitt, *Clays Clay Miner.* **1982**, *30,* 143–149. **DOI:**10.1346/CCMN.1982.0300209
69. J. Ellison, G. Wykoff, A. Paul, R. Mohseni and A. Vasiliev, *Colloid Surface A*. **2014**, *447,* 67–70.
70. A. A. J. Ranchani, V. Parthasarathy, A. A. Devi, B. Meenarathi and R. Anbarasan, *Appl Nanosci.* **2017**, *7,* 577–588. **DOI:**10.1007/s13204-017-0595-6
71. S. Lijuan, H. Jiang, A. Songsong, J. ZHANG, J. ZHENG and R. Dong, *Chinese Journal of Catalysis*. **2013**, *34*, 1378–1385.
72. S. Wunder, F. Polzer, Y. Lu, Y. Mei and M. Ballauff, *The Journal of Physical Chemistry C*. **2010**, *114,* 8814–8820. **DOI:**10.1021/jp101125j
73. S. Cazaux, P. Caselli, A. Tielens, J. Le Bourlot and M. Walmsley: *Journal of Physics: Conference Series, IOP Publishing*. **2005**, pp. 155.
74. H. Hilal, G. Y. M. Nour and A. Zyoud, Book Photodegradation of Methyl orange and phenazo- pyridine HCl with direct solar light using ZnO and activated carbon supported ZnO, 2009.
75. H. Hilal, L. Majjad, N. Zaatar and A. El-Hamouz, *Solid State Sciences*. **2007**, *9,* 9–15. **DOI:**10.1016/j.solidstatesciences.2006.10.001
76. Y. Zhao, E. Abdullayev and Y. Lvov, *IOP Conference Series: Materials Science and Engineering, IOP Publishing*. **2014**, pp. 012043.
77. A. Zainal Abidin, N. H. H. Abu Bakar, E. P. Ng and W. L. Tan, *Journal of Taibah University for Science*. **2017**, *11*, 1070–1079. **DOI:**10.1016/j.jtusci.2017.06.004
78. S. Joseph and B. Mathew, Journal of Molecular Liquids **2015**, *204,* 184–191. **DOI:**10.1016/j.molliq.2015.01.027
79. X. Liu, M. Liang, M. Liu, R. Su, M. Wang, W. Qi and Z. He, *Nanoscale Res Lett*. **2016**, *11,* 440. **DOI:**10.1186/s11671-016-1647-7
80. N. Basavegowda, K. Mishra and Y. R. Lee, *J. Alloy Compd.* 2**017**, *701,* 456–464. **DOI:**10.1016/j.jallcom.2017.01.122

Povzetek

Sintetizirali in okarakterizirali smo nanodelce srebra z vključenimi haloizitnimi nanocevkami (Ag/HNT) in jih uporabili kot katalizator za redukcijo rodamina 6G (Rh6G) in metiloranža (MO). 3-glicidilokiproiltrimetoksisilan in trietil-tetraamin smo uspešno uporabili za kemijsko modifikacijo površine HNT na katero reducirani Ag^+ ioni vezali v obliki nanodelcev (AgNP). Strukturo HNT prekritih z AgNP smo karakterizirali s FTIR, XRD, TEM, FE-SEM ter EDM in pokazali, da so nanodelci srebra veliki 10–15 nm. Katalitsko sposobnost reduciranja Rh6G in MO z Ag/HNT smo spremljali z UV-vis spektroskopijo, s čimer smo lahko primerjali hitrost katalizirane in nekatalizirane reakcije. Konstanta reakcijske hitrosti katalizirane reakcije je znašala za redukcijo Rh6G 0.224 min^{-1}, za redukcijo MO pa 0.222 min^{-1}, medtem ko je bila hitrost nekatalizirane reakcije le 0.049 min^{-1} oziroma 0.014 min^{-1}. Ag/HNT katalizator smo uporabili 6 krat, ne da bi zaznali upad katalitske aktivnosti. Rezultati kažejo možnost obstoja Ag/HNT z izboljšanimi redukcijskimi sposobnostmi, v primeru njihove funkcionalizacije.